Temperate and tropical brown macroalgae thrive, despite decalcification, along natural CO2 gradients

Johnson, VR

Temperate and tropical brown macroalgae thrive, despite decalcification, along natural CO_2 gradients

V I V I E N N E   R .   J O H N S O N *†,   B A Y D E N   D .   R U S S E L L ‡,   K A T H A R I N A   E .   F A B R I C I U S §,
C O L I N   B R O W N L E E †   and   J A S O N   M .   H A L L - S P E N C E R *

*Marine Biology and Ecology Research Centre, University of Plymouth, Plymouth, PL4 8AA, UK, †The Marine Biological Association of the United Kingdom (MBA), The Laboratory, Citadel Hill, Plymouth, PL1 2PB, UK, ‡ Southern Seas Ecology Laboratories, Earth and Environmental Sciences, The University of Adelaide, Adelaide, SA 5005, Australia, § Australian Institute of Marine Science, PMB 3, Townsville, QLD 4810, Australia

Abstract

Predicting the impacts of ocean acidification on coastal ecosystems requires an understanding of the effects on macro-algae and their grazers, as these underpin the ecology of rocky shores. Whilst calcified coralline algae (Rhodophyta) appear to be especially vulnerable to ocean acidification, there is a lack of information concerning calcified brown algae (Phaeophyta), which are not obligate calcifiers but are still important producers of calcium carbonate and organic matter in shallow coastal waters. Here, we compare ecological shifts in subtidal rocky shore systems along CO_2 gradients created by volcanic seeps in the Mediterranean and Papua New Guinea, focussing on abundant macro-algae and grazing sea urchins. In both the temperate and tropical systems the abundances of grazing sea urchins declined dramatically along CO_2 gradients. Temperate and tropical species of the calcifying macroalgal genus *Padina* (Dictyoaceae, Phaeophyta) showed reductions in $CaCO_3$ content with CO_2 enrichment. In contrast to other studies of calcified macroalgae, however, we observed an increase in the abundance of *Padina* spp. in acidified conditions. Reduced sea urchin grazing pressure and significant increases in photosynthetic rates may explain the unexpected success of decalcified *Padina* spp. at elevated levels of CO_2. This is the first study to provide a comparison of ecological changes along CO_2 gradients between temperate and tropical rocky shores. The similarities we found in the responses of *Padina* spp. and sea urchin abundance at several vent systems increases confidence in predictions of the ecological impacts of ocean acidification over a large geographical range.

Keywords: calcification, ocean acidification, photosynthesis, temperate and tropical coastal ecosystems

Received 29 March 2012; revised version received 29 March 2012 and accepted 31 March 2012

Introduction

Rising anthropogenic emissions of CO_2 are rapidly altering ocean chemistry as increasing pCO_2 in seawater has already lowered the mean ocean surface pH by 0.1 units from preindustrial values, with a predicted further decrease of 0.3–0.4 units by 2100 (IPCC (Intergovernmental Panel on Climate Change), 2007). The resulting decrease in calcium carbonate saturation levels compromises the ability of many marine organisms to form shells and skeletons (Orr *et al.*, 2005; Doney *et al.*, 2009). This, in combination with the diverse responses of photosynthetic organisms to increased pCO_2 levels (Russell *et al.*, 2009; Hepburn *et al.*, 2011; Porzio *et al.*, 2011; Johnson *et al.*, 2012), is expected to alter the structure of biological communities along coastlines worldwide (Barry *et al.*, 2011). However,

the potential effects of altered community structure on ecosystem functioning are unclear as the effects of elevated CO_2 levels on organism interactions have only recently begun to be addressed (Diaz-Pulido *et al.*, 2011; Doropoulous *et al.*, 2012).

Seagrasses and many macroalgal species are notably tolerant of, or even benefit from increases in CO_2 (Connell & Russell, 2010; Fabricius *et al.*, 2011; Porzio *et al.*, 2011; Roleda *et al.*, 2011). However, studies from polar, temperate and tropical latitudes have revealed that settlement, calcification, growth and abundance of calcified macroalgae can be negatively affected by increasing CO_2 levels as this lowers carbonate saturation states which can corrode the algal skeletons (Kuffner *et al.*, 2008; Martin *et al.*, 2008; Martin & Gattuso, 2009; Robbins *et al.*, 2009; Russell *et al.*, 2009; Büdenbender *et al.*, 2011; Price *et al.*, 2011; Sinutok *et al.*, 2011; Doropoulous *et al.*, 2012). Increasing concentrations of CO_2 can, on the other hand, enhance productivity and growth in both noncalcified (Kübler *et al.*, 1999; Connell

Correspondence: Jason M. Hall-Spencer, tel. + 44 175 258 4629, fax + 44 175 258 4670, e-mail: jhall-spencer@plymouth.ac.uk

& Russell, 2010) and calcified macroalgae (Reiskind *et al.*, 1988; Semesi *et al.*, 2009).

Understanding the effects of ocean acidification on calcified algae is of a high priority as they play a crucial role in the ecology of coastal ecosystems (Nelson, 2009). Most studies to date have been single species laboratory experiments that last a year at most (Martin & Gattuso, 2009). Such experiments provide important information on species' responses to increased pCO_2 but fail to account for the effects of long-term exposure. They are also unrepresentative of natural ecosystems since, for example, they remove the effects of species interactions (Barry *et al.*, 2011). In contrast to short laboratory experiments, CO_2 gradients in natural settings, where whole ecosystems have been exposed to elevated levels of pCO_2, allow us to investigate changes in the interactions, competition, predation and/or herbivory that involve long-lived metazoan species in benthic marine ecosystems.

Volcanic CO_2 gradients are beginning to reveal the ecological shifts that can be expected to occur with globally increasing atmospheric CO_2 in both temperate (Hall-Spencer *et al.*, 2008) and tropical ecosystems (Fabricius *et al.*, 2011). Work has begun to show the underlying mechanisms that cause ecological shifts along these CO_2 gradients, such as the influence of recruitment success (Cigliano *et al.*, 2010) and the combined physiological effects of temperature and CO_2 (Rodolfo *et al.*, 2011). Drawbacks associated with using this approach include the fact that these are open systems surrounded by waters that are unaffected by the vents, a situation that is unrealistic as the global oceans acidify (Hall-Spencer 2011). Despite such limitations, this mensurative approach provides insights that are complimentary in scope and scale to the prevalent *ex situ* approaches (Wernberg *et al.*, 2012). Here we assess the abundance of herbivores (sea urchins) and the response of brown macroalgae (*Padina* spp.) to increasing levels of CO_2 in natural settings, as interactions between these groups of organisms can drive ecological changes in benthic habitats on temperate (Sala *et al.*, 1998; Hernández, *et al.*, 2008) and tropical shores (McClanahan, 1994; Mumby *et al.*, 2006).

Padina is one of only two genera of Phaeophyta that calcify and is an important producer of calcium carbonate and organic matter in both temperate and tropical shallow waters (Bathurst, 1971; Milliman, 1974). Calcium carbonate is deposited as aragonite needles on the surface of fan-shaped thalli, forming concentric bands of white precipitate (Okazaki *et al.*, 1986). Carbonate production rates of *Padina* sp. in one subtropical system have been calculated to be around 240 $gm^{-2} yr^{-1}$, considerably higher than for other erect calcified algal genera such as *Halimeda* (50 $gm^{-2} yr^{-1}$) and *Penicillus*

(30 $gm^{-2} yr^1$) (Wefer, 1980). Several roles have been suggested for calcification in macroalgae. It is thought to offer structural defence, providing mechanical resistance to herbivores and minimizing grazing damage to tissues (Littler & Littler, 1980; Padilla, 1993), increase the ability for bicarbonate and nutrient assimilation through the generation of protons (McConnaughey & Whelan, 1997), improve photosynthetic performance (McConnaghey, 1998) and provide protection from excess irradiance (Bürger & Schagerl, 2010). Therefore changes in macroalgal calcification as a result of ocean acidification have the potential to alter physiological and ecological fitness, by altering photosynthetic efficiency, thallus rigidity, growth rates and mortality (Nelson, 2009).

Our present knowledge of the effects of ocean acidification on calcified macroalgae is mostly derived from studies investigating the impacts of elevated CO_2 on calcifiers with high magnesium calcite skeletons, such as the family Corallinaceae (Anthony *et al.*, 2008; Kuffner *et al.*, 2008; Martin *et al.*, 2008; Martin & Gattuso, 2009; Semesi *et al.*, 2009; Gao & Zheng, 2010; Büdenbender *et al.*, 2011). The surface seawater saturation state of aragonite (Ω 3–4) is greater than that of high magnesium calcite (Ω 2–3), so algae that precipitate the latter are expected to have more difficulty producing their $CaCO_3$ skeletons under increasing CO_2 than aragonite species (Kleypas *et al.*, 1999) and, as a consequence, aragonitic species have been relatively overlooked. Furthermore, the responses of calcified Phaeophyta are virtually unknown (Porzio *et al.*, 2011). *Padina* spp. are not obligate calcifiers and deposit $CaCO_3$ extracellularly (on the thallus surface), so their response may differ to that of Corallinaceae which are obligate calcifiers with intercellular deposition (within cell walls).

Ocean acidification also has the potential to reduce top-down biological control of benthic biodiversity (Widdicombe & Spicer, 2008). Sea urchins are dominant grazers in many marine habitats and play an important role in controlling the structure and composition of macroalgal communities. They often act as keystone species (Sala *et al.*, 1998) and, as a consequence, reduction in their abundance or removal from an ecosystem can result in rapid colonization of benthic habitats by macroalgae (Villouta *et al.*, 2001; Behrens & Lafferty, 2004). Sea urchins are particularly susceptible to reductions in pH (Miles *et al.*, 2007) and a mean pH of 7.8 appears to be the critical level below which Mediterranean sea urchins do not survive (Hall-Spencer *et al.*, 2008). Adverse impacts of ocean acidification on echinoderms would be likely to have significant consequences at the ecosystem level (Barry *et al.*, 2010; Dupont *et al.*, 2010). It has the potential to release algae from the control of grazing by sea urchins, resulting in

cascade effects throughout benthic food webs, with potentially profound implications for the structure and function of marine communities.

The aim of this study was to survey populations of sea urchins (Echinoidea) and *Padina* spp. (Dictyotaceae) along pH gradients in both temperate and tropical ecosystems, and to measure *in situ* effects of elevated CO_2 on calcification and photosynthesis in this common phaeophyte. We present data on the long-term effects of natural exposure to low pH and high CO_2 on *Padina pavonica* (Linnaeus) Thivy at shallow, volcanic CO_2 seeps on the island of Vulcano, NE Sicily and on *Padina australis* Hauck at comparable seeps in the D'Entrecasteaux Island group, Papua New Guinea. To our knowledge, this is the first study to compare ecological responses to CO_2 gradients in temperate and tropical systems. We observed strikingly similar ecological shifts along both tropical and temperate rocky shores as CO_2 levels increased to those previously recorded at CO_2 vents off Ischia, Italy (Hall-Spencer *et al.*, 2008), with the loss of sea urchins and coralline algae together with an increased abundance of phaeophytes.

Material and methods

Temperate and tropical rocky shore surveys

Padina pavonica was sampled along a stretch of rocky coast off the island of Vulcano (38°25′ N, 14°57′ E, part of the Aeolian Island chain, NE Sicily) in September 2010 and May 2011 (see maps in Johnson *et al.*, 2012). This is a microtidal region where volcanic CO_2 vent activity acidifies the seawater producing a pH gradient ranging from ~8.2 to ~6.8, running parallel to the coast. Within the vent area, three shallow (<0.5 m depth) sampling stations were selected as they lay along a CO_2 gradient, characterized by intermediate to low mean pH (V-S1 pH 8.06, CI = 0.59%; V-S2 pH 7.54, CI = 1.59%; V-S3 pH 7.46, CI = 2.03%, $n = 24–27$). Three reference stations located outside the vent area were selected on the basis of their normal, relatively stable pH (V-R1 pH 8.17, CI = 0.42%; V-R2 pH 8.18, CI = 0.32%; V-R3 pH 8.19, CI = 0.28%, $n = 22–24$). Four additional sampling stations were selected along the gradient, one located between S2 and S3 (at mean pH 7.97, CI = 1.45%, $n = 16$) and three at 20 m intervals between S1 and the end of the gradient (at mean pH 8.08, CI = 0.82%; pH 8.16, CI = 0.33%; pH 8.20, CI = 0.23%, $n = 6–22$) to allow *P. pavonica* and sea urchin abundance surveys to occur along the full length of the CO_2 gradient. Temperature, total alkalinity, salinity and light levels were relatively constant in the shallow subtidal region along this gradient (Johnson *et al.*, 2012).

Padina australis was sampled along the shallow (0.1–0.3 m, below lowest astronomic tide) shore of two sites in Milne Bay Province, Papua New Guinea (9°45′ S, 150°50′ E): Upa-Upasina and Esa'Ala along the north-western and north-eastern coast off Normanby Island (see maps in Fabricius *et al.*, 2011) in April 2011. Tidal range in the region is <1 m. Volcanic CO_2

seeps acidify the seawater, with seeping being most intense near the shore at <0.5 m depth. In these shallow shore zones, reductions in pH were greater than recorded for coral reef habitats by Fabricius *et al.* (2011). Two sampling stations of intermediate to low mean pH were selected at both Upa-Upasina (U-S1 pH 7.78, CI = 0.26%; U-S2 pH 7.49, CI = 0.62%, $n = 7$) and Esa'Ala (E-S1 pH 7.86, CI = 1.30%; E-S2 pH 6.68, CI = 4.53%, $n = 7–9$). Reference stations with normal, relatively stable pH (U-R1 pH 8.31, CI = 0.12%; U-R2 pH 8.22, CI = 0.10%; E-R1 pH 8.19, CI = 0.77%, $n = 6–9$) were chosen several hundred meters away from the seeps at comparable geophysical settings. There was variation in pH at stations exposed to the CO_2 seepage, particularly at Vulcano (stations S2 and S3). This is the result of variable mixing of ambient seawater during calm vs. windy periods and is inherent at CO_2 vent systems (Fabricius *et al.*, 2011; Hoffmann *et al.*, 2011; Kerrison *et al.*, 2011).

At all sites (Vulcano in the Mediterranean, and Upa-Upasina and Esa'Ala in Papua New Guinea), 20 quadrats (50 cm × 50 cm) were placed haphazardly ('blind throws') within 15 × 3 m survey zones (<0.5 m depth) at each station along the CO_2 gradients. Within each quadrat, the percentage cover of *Padina* spp. was estimated and the total number of sea urchins (*Paracentrotus lividus* & *Arbacia lixula* in the Mediterranean, *Diadema* spp. & *Echinometra* sp. in Papua New Guinea) recorded. Visual estimates were conducted by VRJ and JH-S who compared their techniques to minimize inter-observer variability.

Carbonate chemistry measurements

A calibrated pH meter was used to measure pH (NBS scale) at each sampling station at Vulcano (YSI 556 MPS, three-point calibration) and Papua New Guinea (Hach or Oakton, two-point calibration, with readings cross-checked against a Tris buffer seawater standard). Temperature and salinity were also measured alongside each pH reading. We recorded rapid pH fluctuations along this coastal gradient (over 1 unit in under ~4 h at S3 at Vulcano), so the uncertainty inherent in using the NBS scale for seawater measurements (approximately 0.05 pH, Dickson, 2010) was considered acceptable for this study. Mean pH (back-transformed hydrogen ion concentrations) was calculated for each station at Vulcano (pH sampled on several occasions, at various times of the day; September–October 2009, April 2010, July 2010, September–October 2010, May 2011, September–October 2011, $n = 22–27$) and Papua New Guinea (25th and 29th April 2011, $n = 6–9$). Ninety-five percentage confidence intervals were calculated and presented as a percentage of the mean pH.

Total alkalinity (TA) was measured alongside pH to calculate the other parameters constraining the carbonate chemistry of the seawater (Hoppe *et al.*, 2010). At Vulcano, TA was measured at each station, on three separate visits (September 2010, May 2011 and September 2011), from a water sample after 0.2 μm filtration and storage in the dark at 4 °C, using an AS-Alk 2 Total Alkalinity Titrator (Apollo SciTech Inc, Bogart, GA, USA). Total alkalinity data for Papua New Guinea were taken from Fabricius *et al.* (2011). The remaining parameters

of the carbonate system were calculated using the CO2 SYS software (Lewis & Wallace, 1998).

Padina spp. calcium carbonate analysis

Large (>2 cm) *Padina* spp. fronds were collected from each sampling station at Vulcano in the Mediterranean ($n = 30$ per station) and from a reference and high CO_2 station at both Upa-Upasina (U-R1 & U-S1, $n = 15$ per station) and Esa'Ala (E-R1 & E-S2 $n = 5$ per station) in Papua New Guinea. Samples were stored in 70% ethanol until analysis. Calcium carbonate ($CaCO_3$) content of each frond was determined through a weight loss after acidification protocol (Martone, 2010). Fronds were dried, weighed and decalcified in hydrochloric acid (1N) overnight. This resulted in the complete dissolution of a thin layer of $CaCO_3$; the fronds were then redried and reweighed. The $CaCO_3$ content, expressed as a percentage of dry weight, was calculated from the difference between dried mass and decalcified dry mass.

Images of *P. pavonica* aragonite crystals were examined for size and abundance using scanning electron microscopy (JEOL JSM 5600 LV: JEOL Ltd., Tokoyo, Japan). Three fronds from each station were fixed in glutaraldehyde for 1–2 h, and then stored in $1\times$ PBS buffer (phosphate buffered saline) until examination. As the size and number of crystals has been reported to vary with age of frond segment (Hillis-Colinvaux, 1980), we only compared the apical segments of *P. pavonica* fronds between stations. Prior to viewing under the SEM, samples were air dried, mounted on aluminium stubs with carbon adhesive tape and coated in gold. For each of the 18 samples, five images were taken at random locations (using image coordinates and random number generator) over calcified regions of the apical surface only (see images in Fig. 4) and the average length and width of 10 randomly selected crystals per image was measured digitally using Image J software (v 1.43; National Institutes of Health, Bethesda, MD, USA). In addition, for each image, the number of crystals within a randomly selected 5 μm $\times$ 5 μm area were counted and averaged for each frond.

Photosynthesis in Padina pavonica

Photosynthetic capacity and performance of *P. pavonica* at Vulcano was investigated through measurements of photosynthetic pigment (Chl *a* and c_1+c_2) concentrations and Chl *a* fluorescence respectively. These physiological measurements were performed in summer months (May and September) when algal productivity is high. For pigment analysis, fronds were collected from each sampling site at Vulcano in September 2010 and September 2011($n = 40$ per station), rinsed in distilled water and frozen for transportation back to the laboratory. Fronds were collected between 8:00 and 10:00 hours to avoid the confounding effect of light intensity, in particularly mid-day photoinhibition, on chlorophyll content (Häder *et al.*, 1996). To prevent chlorophyll degradation during storage, samples were kept at -20 °C in the dark during the sampling period on Vulcano and at -80 °C when longer periods occurred before analysis. Chlorophyll was extracted from all samples within <2 weeks of sampling.

Prior to extraction, fronds (~0.70 g samples) were homogenized in 90% acetone by pestle and mortar. Chlorophyll was extracted in 90% acetone at 4 °C for 24 h in the dark. The absorbance of each sample at 630, 664 and 750 nm (background absorbance) was measured (three replicate readings were taken from each sample to obtain an average) using a Cecil CE2011 spectrophotometer (Cecil Instruments Ltd, Cambridge, UK). The concentration of chlorophyll *a* and *c* ($c_1 + c_2$) in the sample was calculated using the equations of Ritchie (2006). The volume of the solvent (in weight g^{-1}) and the weight of the frond were then used to provide a final calculated reading of chlorophyll (μg mg^{-2} fresh weight). Values for both September sampling periods were pooled to calculate a mean for each station.

In May 2011, the effective quantum yield (Y) and relative electron transport rates (*r*ETR) of freshly collected, light-adapted fronds ($n = 6$ per station, stored in seawater from site of collection), were measured in small dishes using a Diving-PAM fluorometer (Heinz Walz GmbH, Effeltrich, Germany) in a dimly lit room.

$$Y = F'_m - F'_t/F'_m$$
$$r\text{ETR} = Y \times \text{PAR} \times 0.5$$

where; F'_m = maximum florescence yield of light adapted fronds, F_t = steady-state level of flourescence under illumination at time t (Genty *et al.*, 1989), PAR = photosynthetic active radiation and 0.5 is a constant assuming both PSI and PSII absorb equal amounts of the incoming photons (Beer *et al.*, 1998).

Rapid light curves (RLC) were applied to assess the light saturation behaviour of individual, whole fronds across each of the six sampling stations in Vulcano. Rapid light curves data can be useful for assessing photosynthetic capacity and potential over a wide range of ambient light intensities (Ralph & Gademan, 2005). The Diving-PAM was set to deliver red pulse-modulated light at 655 nm followed by steps of actinic light from 1 to 3344 μmol photons m^{-2}s^{-1} delivered every 20 s over a period of 160 s (other settings: gain = 4, actinic light factor = 0.5, light curve intensity y = 5, saturation width = 0.8, saturation intensity = 3, signal damping = 2).

Statistical analyses

To test for significant effects of mean pH on variations in *Padina* spp. we used generalized linear models (GLM), with pH as the explanatory variable and Site (Vulcano, Upa Upasina and Esa'Ala) as a covariate. Data were averaged across stations and transformed where necessary to approximate normality and equal variance. For count data with many zeroes (e.g., sea urchin abundances) or overdispersed data, a quasi-poisson link function was used, whereas for proportional, ETR and yield data, a quasi-binomial link function, and for the remaining data the Gaussian link function were used. All statistical
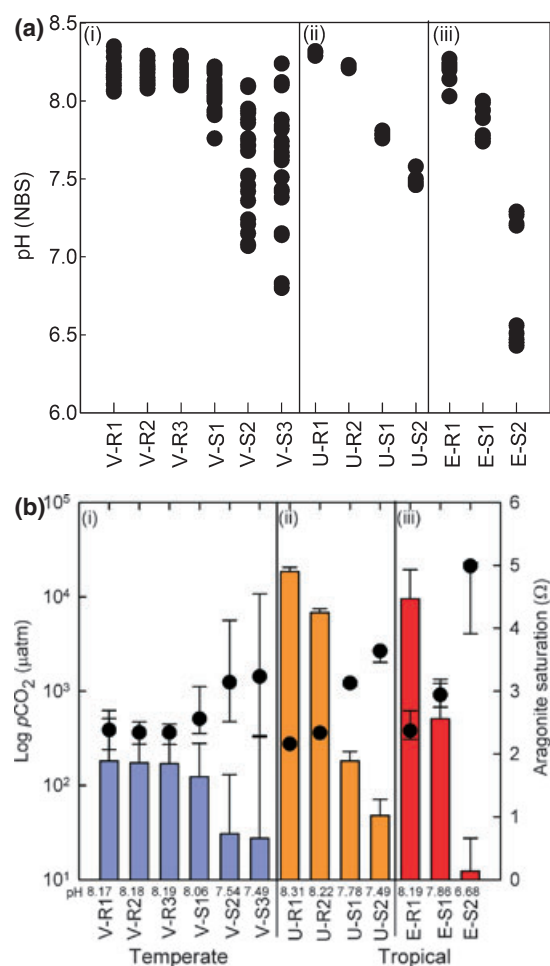
Fig. 1 (a) Range in pH$_{NBS}$ (<0.5 m water depth) across CO$_2$ gradients in (i) Vulcano (Sicily; $n = 22$–27 per station) (ii) Upa-Upasina (Papua New Guinea; $n = 6$ per station) (iii) Esa'Ala (Papua New Guinea; $n = 7$ & S2, $n = 9$). 'R' denotes reference stations, 'S' denotes elevated CO$_2$ stations. (b) Range in pCO$_2$ (scatter plot) and aragonite saturation (bar chart) across CO$_2$ gradients in (i) Vulcano, (ii) Upa-Upasina and (iii) Esa'Ala. Dots and bars = median values, upper & lower limits = maximum and minimum values, respectively.

analyses were performed using R (R Development Core Team, 2011).

Results

Seawater chemistry

The mean pH of the reference stations in all three systems ranged from 8.17 to 8.31, whereas the mean pH at the seep stations ranged from 8.06 to 6.68, with increasing variance towards lower values (Fig. 1a). Carbonate chemistry parameters for each sampling station are presented in the supplementary material (Table S1). The range in pCO$_2$ and aragonite saturation along the
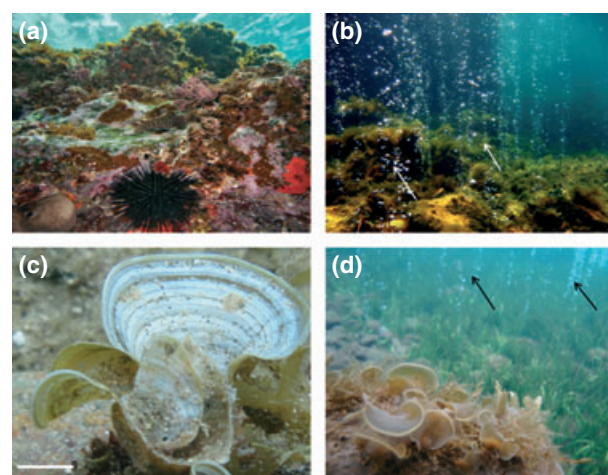

Fig. 2 Images showing an urchin and coralline algae dominated rocky shore under ambient CO$_2$ (a) in Ischia, Italy (photograph by David Liittschwager, National Geographic) and the proliferation of Phaeophyta at elevated CO$_2$ at vent sites in Ischia (photograph by Luca Tiberti, Associazione Nemo) (b). *Padina australis* showing normal calcification at tropical (Papua New Guinea) reference station, Esa'Ala R1 (c; scale bar = 1 cm) and visibly low calcification at Esa'Ala S1 (d). Arrows indicate CO$_2$ vent bubbles.

gradients is displayed in Fig.1b. The median pCO$_2$ levels (calculated from median pH and mean TA) were lowest at the reference stations (276–388 µatm) and increased with proximity to the seeps, with the highest values recorded at V-S3 (1428 µatm), U-S2 (2665 µatm) and E-S2 (23 095 µatm). The highest median values for pCO$_2$ and DIC were found at V-S3 (1428 µatm and 3.79 mmol kg^{-1} respectively), U-S2 (2665 µatm and 2.03 mmol kg^{-1}) and E-S2 (23 095 µatm and 2.85 mmol kg^{-1}). Aragonite saturation decreased with increasing levels of CO$_2$ (Fig.1b) and periods of undersaturation occurred at stations V-S2, V-S3, U-S2 and E-S2.

Padina spp. and sea urchin abundances

There were dramatic ecological shifts along all three volcanic seeps as CO$_2$ levels increased. We observed a loss of sea urchins and coralline algae together with an increased abundance of phaeophytes that was strikingly similar to that recorded at CO$_2$ vents in Ischia, Italy (Fig 2a and b). These shifts were detected at median pCO$_2$ levels of 510 µatm (median pH 8.08), 1218 µatm (median pH 7.78) and 914 µatm (median pH 7.89) along the gradients at Vulcano, Upa Upasina and Esa'Ala respectively (Fig. 3a). Benthic cover of *Padina* spp. increased with rising CO$_2$ and was twofold–threefold greater in the highest CO$_2$ stations (V-S3, U-S2 & E-S2) relative to the reference stations (Fig. 3a). We
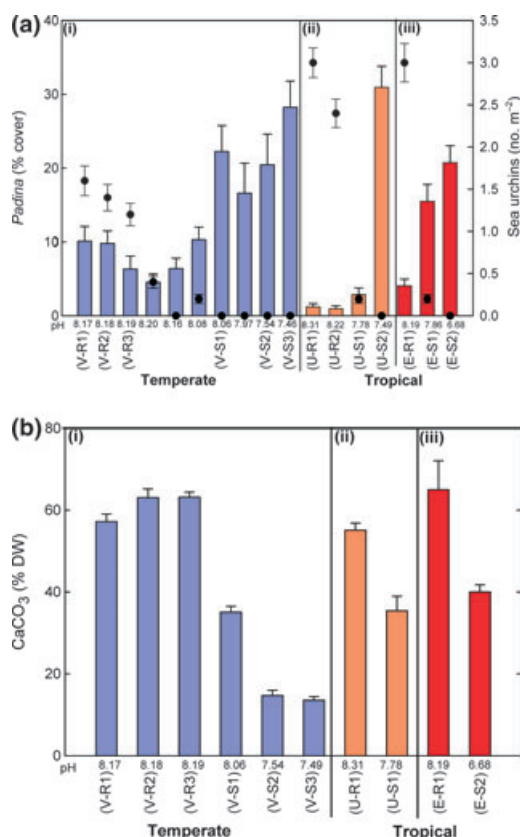
Table 1 Changes in (a) *Padina* spp. cover, (b) urchin abundances and (c) $CaCO_3$ content of *Padina* spp. fronds, along the three pH gradients at Esa'Ala, Upa-Upasina and Vulcano. Generalized linear model outputs. Data in bold indicate significant effect of pH ($P < 0.05$)

	Estimate	SE	t	P
(a)				
Region.Esa	14.03	4.31	3.26	0.008
Region.Upa	22.83	8.74	2.61	0.024
Region.Vul	17.05	7.32	2.33	0.040
Region.Esa: pH	−1.38	0.57	−2.43	**0.033**
Region.Upa: pH	−4.28	0.96	−4.48	**0.001**
Region.Vul: pH	−3.48	0.74	−4.70	**0.001**
(b)				
Region.Esa	−27.82	8.56	−3.25	0.006
Region.Upa	−0.31	0.51	−0.61	0.553
Region.Vul	−0.66	0.46	−1.43	0.176
pH	3.40	1.06	3.22	**0.007**
(c)				
Region.Esa	−5.07	2.19	−2.32	0.082
Region.Upa	−7.38	7.03	−1.05	0.353
Region.Vul	−21.20	4.83	−4.39	0.012
Region.Esa: pH	0.70	0.29	2.38	0.076
Region.Upa: pH	1.52	0.83	1.84	0.140
Region.Vul: pH	3.25	0.54	6.06	**0.004**

Fig. 3 (a) Mean percentage cover (histogram + SE) of *Padina* spp. and abundance of sea urchins (mean ± SE) along CO_2 gradients at (i) Vulcano (ii) Upa-Upasina (iii) Esa'Ala ($n = 20$ quadrats per station). Mean pH ($n = 6$–27 per station) of each station indicated. (b) Mean (+SE) $CaCO_3$ content of *Padina* spp. along CO_2 gradients at (i) Vulcano ($n = 30$ per station), (ii) Upa-Upasina ($n = 15$ per station) and iii) Esa'Ala) ($n = 5$ per station).

detected a significant relationship between pH and both *Padina* spp. benthic cover and sea urchin abundance at all three gradients (GLM: Table 1). In contrast to *Padina* spp., sea urchin abundance was greatest at the reference stations and decreased with declining pH at all three gradients (Fig. 3a; Table 1). Sea urchins were absent at stations with the highest levels of pCO_2 (V-S1-S3, U-S2, E-S2).

Changes in Padina spp.; CaCO₃ content, crystal structure and photophysiology along the CO₂ gradients

We found that the $CaCO_3$ content in *Padina* spp. fronds was significantly related to pH at Vulcano only (as smaller sample sizes were taken at Upa-Upasina and Esa'Ala; Fig. 3b, Table 1). At Vulcano, $CaCO_3$ content in *P. pavonica* was highest at the reference stations (57–63%) and decreased significantly in the CO_2 enriched stations; S1 (35% ±1.4), S2 (15% ±1.3) and S3 (14% ±0.9). Analysis of *P. australis* from Upa-Upasina in Papua New Guinea also

revealed a large reduction in $CaCO_3$ content from 55% ±1.7 at the reference station (U-R1) to 35% ±3.6 at the intermediate station (U-S1). At Esa'Ala, $CaCO_3$ content was considerably greater in fronds from the reference station (E-R1: 66% ±7.1) compared with those from the highest CO_2 exposure station (E-S2: 40% ±1.8).

The abundance and morphometric data of the aragonite crystals on the surface of *P. pavonica* fronds are presented in the supplementary material (Table S2). Over the thin calcified bands in the apical regions we detected a significant increase in crystal abundances with declining pH (GLM: slope of square root transformed data = −0.23 ± 0.077, $t = -2.99$, $P = 0.037$) and a reduction in the width of crystals (slope = 0.23 ± 0.067, $t = 3.42$, $P = 0.026$), but no effect on crystal length ($P = 0.85$).

The content of both chlorophyll *a* and chlorophyll *c* in *P. pavonica* was significantly related to pH (Fig. 4, GLM: slope = −0.24 ± 0.065, $t = -3.78$, $P = 0.019$; slope = −0.028 ± 0.0055, $t = -5.21$, $P = 0.006$, for chlorophyll *a* and *c* respectively). Both the chlorophyll *a* and *c* content increased with declining pH (Chl *c*: V-S1 = 0.05 mg g^{-1}fw ± 0.002, V-S2 = 0.06 mg g^{-1} fw ± 0.002, V-S3 = 0.07 mg g^{-1} fw ± 0.003 compared with those in the reference stations: V-R1 = 0.04 mg g^{-1} fw ± 0.002, V-R2 = 0.04 mg g^{-1} fw ± 0.004, V-R3 = 0.04 mg g^{-1} fw ± 0.003).
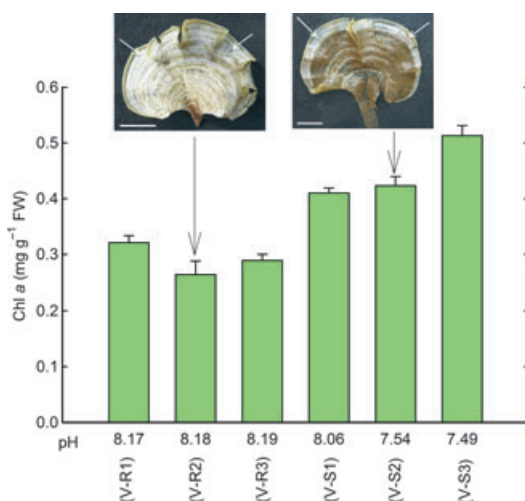
Fig. 4 Mean (+ SE) chl *a* content in *P. pavonica* fronds along the Vulcano CO$_2$ gradient (*n* = 40 per station). Images illustrate changes in CaCO$_3$ deposition on *P. pavonica* frond surfaces at V-R2 and V-S2 along the Vulcano CO$_2$ gradient. All thalli at V-R1- V-R3 were heavily calcified, all thalli at S1–S3 were more lightly calcified, calcification appears to be limited to thin bands along apical regions (scale bar = 1 cm). Arrows indicate locations of SEM analyses.
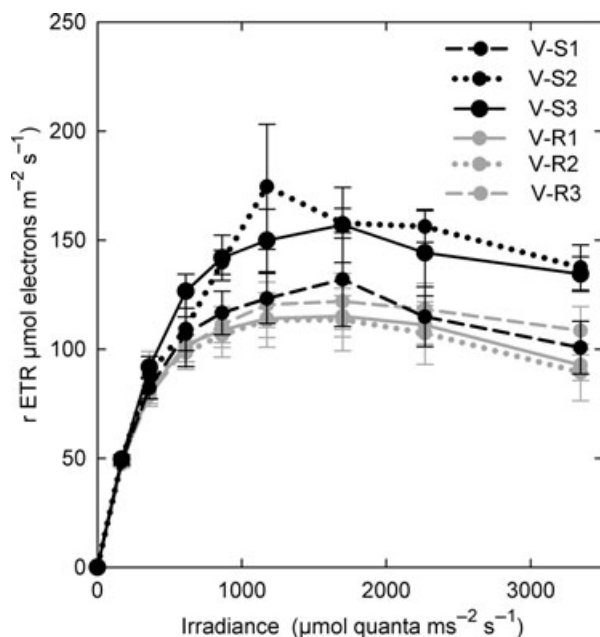

Fig. 5 Rapid light curves of *P. pavonica* along the Vulcano CO$_2$ gradient, showing the mean (± SE) relative electron transport rates (*r*ETR) per station (*n* = 5 for V-R3 + V-S3, *n* = 6 for all other stations) at increasing irradiance.

The differences observed in the photosynthetic responses of *P. pavonica* to increased CO$_2$ are presented in a rapid light curve in Fig. 5. The *r*ETR max values

significantly increased with declining pH (GLM: slope on fourth-root transformed data = −0.54 ± 0.091, *t* = −5.97, *P* = 0.004). We also found that the *r*ETRs recorded at supersaturating irradiance; 3344 μmol quanta m^{-2} s^{-1} were significantly related to pH (slope on fourth-root transformed data = −0.49 ± 0.098, *t* = −4.95, *P* = 0.008) where the greatest values were recorded at S2 and S3 (137.43 μmol electrons m^{-2} s^{-1} ± 10.12, 134.45 ± 7.97 respectively), however no significant relationship between pH and the *r*ETRs under a subsaturating irradiance (360 μmol quanta m^{-2} s^{-1}) could be detected (slope on fourth-root transformed data = −0.12 ± 0.049, *t* = −2.55, *P* = 0.063). We also failed to detect a significant relationship between pH and the photochemical efficiencies (*Fv/Fm*) of *P. pavonica* (*P* = 0.35).

Discussion

To our knowledge, this is the first *in situ* observation of the changes of both grazers and macroalgae along gradients of increasing CO$_2$. It is also the first to provide a comparison of ecological changes along CO$_2$ gradients between temperate and tropical rocky shores. This study reveals dramatic shifts in benthic community structure that were strikingly similar to those documented at another CO$_2$ vent site in Italy (Hall-Spencer *et al.*, 2008). Along both temperate and tropical rocky shores there was a reduction in sea urchin abundances alongside a proliferation of *Padina* spp., as CO$_2$ levels increased. We propose that the elevated CO$_2$ levels may influence algal-grazer dynamics as species assemblages change, causing profound structural and functional changes in rocky shore habitats. The changes in benthic community composition were detected at threshold *p*CO$_2$ levels of ~500 μatm in Sicily and therefore, according to climate change predictions (IPCC (Intergovernmental Panel on Climate Change), 2007), indicate that we may begin to witness these ecological shifts occurring in temperate rocky shores from around the midpoint of this century. Threshold values of *p*CO$_2$ for the rocky shore shifts in Papua New Guinea were considerably higher (>900 μatm) than those in Sicily, this may be because of the relatively limited number of midrange CO$_2$ enriched stations sampled in Papua New Guinea. Investigating the benthos at more intermediate levels of CO$_2$ may have revealed lower threshold values for ecological shifts, similar to those in Sicily.

Unexpected responses of Padina spp. to elevated CO$_2$

Our present knowledge concerning the impacts of ocean acidification has raised concern for the future

success of calcified macroalgae under conditions of high CO_2. Previous investigations at CO_2 vent seeps have observed dramatic reductions in the abundance of calcified macroalgae (Hall-Spencer *et al.*, 2008; Martin *et al.*, 2008; Fabricius *et al.*, 2011). The results from this investigation, however, indicate that some calcified algae may thrive as the oceans acidify despite expected reductions in calcification. We discovered that tropical and temperate *Padina* spp. can proliferate with CO_2 enrichment, as similarly recorded for some genera of fleshy macroalgae (Hall-Spencer *et al.*, 2008; Fabricius *et al.*, 2011; Porzio *et al.*, 2011). That such algae are abundant at CO_2 vents may not, however, necessarily imply that they will be winners in a high CO_2 world as they can recruit from outside the vent areas; new work on seagrasses at volcanic vents reveal that chronic exposure to increased CO_2 levels adversely affects their ability to defend themselves with phenolic compounds (Arnold *et al.*, in press).

In both *P. pavonica* and *P. australis*, the content of $CaCO_3$ in thalli decreased with reductions in pH. This is consistent with other calcification studies on aragonitic macroalgae (Price *et al.*, 2011; Sinutok *et al.*, 2011) and high magnesium calcitic macroalgae (Martin & Gattuso, 2009; Semesi *et al.*, 2009). Reductions in $CaCO_3$ content implies that *Padina* spp. herbivore defence may be compromised under low pH, potentially leading to an increase in grazing mortality and reduction in benthic cover. This was not, however, reflected *in situ*. Sea urchins are major grazers on *Padina* spp. and their presence can cause significant reductions in the abundance of these algae in the Mediterranean (Hereu, 2006) and in the tropics (Sammarco, 1982). Our recorded absence of sea urchins in the CO_2 enriched areas may be one explanation for the proliferation of *Padina* spp., as it becomes released from the top-down control by these keystone grazers. This effect of sea urchin removal has been observed in other *Padina* sp. populations (Sammarco *et al.*, 1974) and across other Phaeophyte assemblages (Leinaas & Christie, 1996; Ling *et al.*, 2010). *In situ* manipulations, such as those carried out on grazing gastropods by Rodolfo *et al.* (2011), are required to test the cause of our observed correlations.

Photosynthetic response of Padina pavonica to elevated CO_2

Increased productivity with elevated CO_2 may also contribute to the success of *Padina* at low pH. Laboratory studies of other calcified macroalgae have revealed declines in photosynthetic pigments in high CO_2/low pH treatments (Gao & Zheng, 2010; Sinutok *et al.*, 2011) which are indicative of chlorophyll degradation, a reduction in photosynthetic unit size and/or a

reduction in PSII reaction centres (Sinutok *et al.*, 2011). Our data, however, show the opposite of the findings from these laboratory studies. We found that Chl *a* and Chl *c* content in *P. pavonica* was greater in the CO_2 enriched stations indicating an increase in photosynthetic capacity under conditions of higher CO_2. A possible cause for the lower Chl *a* content ($\mu g\ mg^{-2}$) in fronds from ambient pH may be because of the higher $CaCO_3$ contents relative to those in low pH which have undergone decalcification. In this case however, CO_2 levels appear to be a more likely cause for the variations as fronds from S2 and S3 shared similar $CaCO_3$ contents, yet Chl *a* content was higher in S3 relative to S2.

It has been speculated that pH stress may negatively impact photosynthetic performance through the disruption of the CO_2 accumulating pathway at the site of Rubisco, or interference with electron transport (Anthony *et al.*, 2008). This has been supported through laboratory experiments with *Halimeda* spp. which have demonstrated declines in photosynthetic efficiency (maximum quantum yield; Fv/Fm) (Sinutok *et al.*, 2011) and response (rETR$_{max}$) (Price *et al.*, 2011) under elevated CO_2. In contrast, we did not observe significant effect of pH on photosynthetic efficiency (Fv/Fm), along gradients of CO_2. Indeed, we found a significant effect on the *in situ* photosynthetic responses of *P. pavonica* with CO_2 enrichment (increases in rETR$_{max}$ and mean rETR$_{max}$ at supersaturating irradiance). Whilst some species of *Padina* are thought to possess carbon concentrating mechanisms (Raven *et al.*, 2002; Enríquez & Rodríguez, 2006) *P. pavonica* is not believed to be carbon-saturated in ambient seawater and, at times, has been shown to utilize more inorganic carbon if it is provided as CO_2 (Einav *et al.*, 1995). The positive photosynthetic response of *P. pavonica* to CO_2 enrichment therefore indicates a direct enhancement of carbon fixation along the gradient. Increased photosynthetic activity at high CO_2 has also been observed in other calcified macroalgae (Reiskind *et al.*, 1988; Semesi *et al.*, 2009) and noncalcified macroalgae (Kübler *et al.*, 1999; Connell & Russell, 2010; Russell *et al.*, 2011b). As our photosynthetic measurements are from one season we cannot assess whether the photosynthetic responses of *P.pavonica* vary seasonally; these data provide a snapshot of responses along gradients of increasing CO_2.

It has been established that photosynthesis can stimulate calcification in algae (Borowitzka, 1982; Gattuso *et al.*, 1999). Okazaki *et al.* (1986) showed that aragonite deposition in *Padina* begins in the intracellular space formed by the infolded apical margin of the thallus and, since chloroplasts also occur in this region, the authors suggest that this may indicate a relationship between the initiation of calcification and photosynthesis. Photosynthesis-induced calcification has also been

demonstrated in the interutricular spaces of the aragonitic genus *Halimeda* (Borowitzka, 1989). Increased $CaCO_3$ dissolution in lower pH may therefore be offset by the increased photosynthesis in those regions with chloroplasts. This may help to explain why we found that even in the lowest pH conditions, *P. pavonica* and *P. australis* were still able to calcify, seemingly from the enhancement of photosynthesis under high levels of CO_2. Alternatively, the high pH variability in the vent zone, caused by transient exposure to ambient pH conditions (i.e., periods of high winds increasing the mixing of vent waters with surrounding high pH seawater), has the potential to buffer the effects of acidification by relieving physiological stress (Hoffmann *et al.*, 2011).

Implications of elevated CO_2 on Padina spp. calcification

There is a lack of laboratory evidence of the effects of low pH on *Padina* spp. calcification to confirm whether decreased calcification is a direct response to reduced pH as opposed to, for example, the reduced grazing pressure in this *in situ* experiment. An investigation of Caribbean *Padina* sp. (Lewis *et al.*, 1987) however, revealed that in heavily grazed areas the algae existed in the form of an uncalcified turf whereas in areas of low grazing activity it grew as calcified, foliose blades. The fact that these algae still calcify when grazing intensity is low suggests that the reduced calcification recorded in this study may indeed be a direct response to lowered pH and not the changes in grazing pressure. It has been suggested that calcium carbonate crystal morphology and abundance may be associated with seawater chemistry: thinner, more abundant crystals have been shown to indicate reduced pH conditions as crystallization events are thought to be initiated and terminated more frequently (Robbins *et al.*, 2009; Sinutok *et al.*, 2011). Over the thin calcified band in the apical region of *P. pavonica* fronds in the CO_2 enriched stations, we recorded more abundant aragonite crystals than in the reference stations and we also observed a decreasing trend of crystal width with increasing levels of CO_2. These results therefore support the theory of pH dependent changes in calcium carbonate crystal morphology and deposition in calcified macroalgae. The implications of changes in *Padina* spp. biocalcification on thallus rigidity, dissolution rates and overall sediment budgets however, need further investigation.

CO_2 vent systems as proxies for ocean acidification

Volcanic vent sites can have highly variable CO_2 levels, with steep gradients in pH and carbonate saturation, so caution is required in using information derived from vent studies in projecting future high-CO_2 scenarios (Riebesell, 2008; Gazeau *et al.*, 2011). Variability in CO_2 levels was seldom considered in the early stages of ocean acidification research, as perturbation experiments mainly investigated the responses of organisms to constant low pH, yet the pH of coastal systems is highly variable with macroalgal communities that can experience diurnal fluctuations of pH 7.5–9.0 (Middelboe & Hansen, 2007; Hoffmann *et al.*, 2011). Volcanic vent systems are useful as they can reveal ecological responses to long-term moderate increases in CO_2 levels that retain natural pH variability (Fabricius *et al.*, 2011; Kerrison *et al.*, 2011). They are also useful for examining response boundaries and determining which organisms are the most resistant to chronic exposures to elevated CO_2 levels (Barry *et al.*, 2010). Communities of organisms exposed to decades of high CO_2 levels provide insights into what to expect in areas that are expected to receive higher than average levels of CO_2, such as areas that may be exposed to CO_2 leaks following subseabed sequestration (Blackford *et al.*, 2009), those with enhanced acidification due to eutrophication events or hypoxic conditions (Brewer & Peltzer, 2009; Cai *et al.*, 2011) or those areas where CO_2-rich waters well-up from the deep into coastal systems (Feely *et al.*, 2008).

Although CO_2 vent systems are much larger and longer lasting than the mesocosm and aquarium experiments that have taken place to date, they still only affect relatively small areas of the seabed. Being open systems, their ecology is affected by surrounding areas that have lower CO_2 levels, allowing recruitment and migration of organisms from unaffected habitats (Cigliano *et al.*, 2010; Hall-Spencer, 2011). Thus CO_2 vent systems cannot mimic the effects of global acidification, they are too small and ephemeral, but they augment predictions based on laboratory and modelling experiments since they show long-term responses of coastal systems to increases in CO_2 levels at a variety of locations worldwide (Wernberg *et al.*, 2012).

Implications of findings

Our study shows that certain calcified phaeophytes could be amongst the ecological winners under ocean acidification scenarios, alongside fleshy macroalgae (Kübler *et al.*, 1999; Porzio *et al.*, 2011; Raven, 2011). This work adds to evidence for proliferation of phaeophytes in a high-CO_2 world (Hall-Spencer *et al.*, 2008; Connell & Russell, 2010; Diaz-Pulido *et al.*, 2011; Russell *et al.*, 2011b) and has potentially profound consequences for the structure, function and resilience of a variety of benthic ecosystems globally (McManus &

Polsenberg, 2004; Harries *et al.*, 2007; Russell *et al.*, 2009). Indeed, the structure and function of ecosystems under future conditions is likely to represent changes to the balance between productivity and consumption (Connell *et al.*, 2011).

Large differences in the impacts of CO_2 enrichment between *Padina* spp. and other calcified species have been made apparent by this study. This highlights the importance of studying a wide range of genera to better inform global predictions of the impacts of ocean acidification on marine ecosystems (Russell *et al.*, 2011a). This study has demonstrated that the response of *Padina* spp. to CO_2 enrichment is complex and potentially multifactorial. An *in situ*, ecosystem based approach, incorporating multispecies interactions, provides more accurate insights into the responses of marine organisms, highlighting the importance of natural CO_2 gradients as a valuable tool in the study of ocean acidification. The similarities we found in the responses of *Padina* spp. and sea urchin abundance at several vent systems increases the robustness of our predictions over a large geographical range. Similar comparisons should be adopted for other marine biota in future ocean acidification studies.

Acknowledgements

References

Anthony KRN, Kline DI, Diaz-Pulido G, Dove S, Hoegh-Guldberg O (2008) Ocean acidification causes bleaching and productivity loss in coral reef builders. *Proceedings of the National Academy of Sciences*, **105**, 17442–17446.

Arnold T, Mealey C, Leahey H *et al.* (in press) Ocean acidification and the loss of protective phenolics in seagrasses. *PLoS ONE*, doi: 10.1371/journal.pone.0035107.

Barry JP, Hall-Spencer JM, Tyrrell T (2010) *In situ* perturbation experiments: natural venting sites, spatial/temporal gradients in ocean pH, manipulative *in situ* *p*(CO_2) perturbations. In: *Guide to Best Practices for Ocean Acidification Research and Data Reporting* (eds Riebesell U, Fabry VJ, Hansson L, Gattuso J-P), pp. 123–136. Publications Office of the European Union, Luxembourg.

Barry JP, Widdicombe S, Hall-Spencer JM (2011). Effects of ocean acidification on marine biodiversity and ecosystem function. In: *Ocean Acidification* (eds Gattuso J-L, Hansson L), pp. 192–209. Oxford University Press, Oxford. Chapter 10.

Bathurst RGC (1971) *Carbonate Sediments and their Diagenesis*, pp. 1–620. Elsevier, Amsterdam, the Netherlands.

Beer S, Vilenkin B, Weil A, Veste M, Susel L, Eshel A (1998) Measuring photosynthetic rates in seagrasses by pulse amplitude modulated (PAM) fluorometry. *Marine Ecology Progress Series*, **174**, 293–300.

Behrens MD, Lafferty KD (2004) Effects of marine reserves and urchin disease on southern Californian rocky reef communities. *Marine Ecology Progress Series*, **279**, 129–139.

Blackford J, Jones N, Proctor R, Holt R, Widdicombe S, Lowe D, Rees A (2009) An initial assessment of the potential environmental impact of CO_2 escape from marine carbon capture and storage systems. *Proceedings of the Institution of Mechanical Engineers Part B- Journal of Engineering Manufacture*, **223**, 269–280.

Borowitzka MA (1982) Mechanisms in algal calcification. *Progress in Phycological Research*, **1**, 137–177.

Borowitzka MA (1989) Carbonate calcification in algae- initiation and control. In: *Biomineralisation* (eds Mann S, Webb J, Williams R), pp. 137–177, vol. 1, Springer-Verlag, New York.

Brewer PG, Peltzer ET (2009) Limits to marine life. *Science*, **324**, 347–348.

Büdenbender J, Riebesell U, Form A (2011) Calcification of the Artic coralline red algae *Lithothamnion glaciale* in response to elevated CO_2. *Marine Ecology Progress Series*, **441**, 79–87.

Bürger K, Schagerl M (2010) Morphological studies of the brown alga *Padina pavonica* (L.) Thivy. Unpublished master thesis, Department of Marine Biology, University of Vienna, Vienna, Austria.

Cai W-J, Hu X, Huang W-J *et al.* (2011) Acidification of subsurface coastal waters enhanced by eutrophication. *Nature Geoscience*, **4**, 766–770.

Cigliano M, Gambi MC, Rodolfo M, etalpa R, Patti FP, Hall-Spencer JM (2010) Effects of ocean acidification on invertebrate settlement at volcanic CO_2 vents. *Marine Biology*, **157**, 2489–2502.

Connell SD, Russell BD (2010) The direct effects of increasing CO_2 and temperature on non-calcifying organisms: increasing the potential for phase shifts in kelp forests. *Proceedings of the Royal Society of London, B*, **277**, 1409–1415.

Connell SD, Russell BD, Irving AD (2011) Can strong consumer and producer effects be reconciled to better forecast 'catastrophic' phase-shifts in marine ecosystems? *Journal of Experimental Marine Biology and Ecology*, **400**, 296–301.

Diaz-Pulido G, Gouezo M, Tilbrook B, Dove S, Anthony KRN (2011) High CO_2 enhances the competitive strengths of seaweeds over coral. *Ecology Letters*, **14**, 156–162.

Dickson AG (1990) Standard potential of the (AgCl + 1/2 H_2= Ag + HCl(aq)) cell and the association of bisulfate ion in synthetic sea water from 273.15 to 318.15 K. *Journal of Chemical Thermodynamics*, **22**, 113–127.

Dickson AG (2010) The carbon dioxide system in seawater: equilibrium chemistry and measurements. In: *Guide to Best Practises for Ocean Acidification Research and Data Reporting* (eds Riebesell U, Fabry VJ, Hansson L, Gattuso JP), pp. 17–52. Publications Office of the European Union, Luxembourg.

Doney SC, Fabry VJ, Feely RA, Kleypas JA (2009) Ocean acidification: the other CO_2 problem. *Annual Review of Marine Science*, **1**, 169–92.

Doropoulous C, Ward S, Diaz-Pulido G, Hoegh-Guldberg O, Mumby PJ (2012) Ocean acidification reduces coral recruitment by disrupting intimate larval-algal settlement interactions. *Ecology Letters*, **15**, 338–346, doi: 10.1111/j.1461-0248.2012.01743.

Dupont S, Ortega-Martinez O, Thorndyke M (2010) Impact of near-future ocean acidification on echinoderms. *Ecotoxicology*, **19**, 449–462.

Einav R, Breckle S, Beer S (1995) Ecophysiological adaptation strategies of some intertidal marine macroalgae of the Israeli Mediterranean coast. *Marine Ecology Progress Series*, **125**, 219–228.

Enríquez S, Rodríguez R (2006) Effect of water flow on the photosynthesis of three marine macrophytes from a fringing-reef lagoon. *Marine Ecology Progress Series*, **323**, 119–132.

Fabricius KE, Langdon C, Uthicke S *et al.* (2011) Losers and winners in coral reefs acclimatized to elevated carbon dioxide concentrations. *Nature Climate Change*, **1**, 165–169.

Feely RA, Sabine CL, Hernandez-Ayon JM, Ianson D, Hales B (2008) Evidence for upwelling of corrosive "acidified" water onto the continental shelf. *Science*, **320**, 1490–1492.

Gao K, Zheng Y (2010) Combined effects of ocean acidification and solar UV radiation on photosynthesis, growth, pigmentation and calcification of the coralline alga *Corallina sessilis* (Rhodophyta). *Global Change Biology*, **16**, 2388–2398.

Gattuso JP, Allemand D, Frankignoulle M (1999) Photosynthesis and calcification at cellular, organismal and community levels in coral reefs: a review on interactions and control by carbonate chemistry. *American Zoologist*, **39**, 160–183.

Gazeau F, Martin S, Hansson L, Gattuso JP (2011) *Ocean acidification in the coastal zone.* In: Inprint Issue 3, Land-Ocean Interactions in the Coastal Zone (LOCIZ), Germany.

Genty B, Briantais JM, Baker NR (1989) The relationship between the quantum yield of photosynthetic electron-transport and quenching of chlorophyll fluorescence. *Biochimica Et Biophysica Acta*, **990**, 87–92.

Häder DP, Lebert M, Mercado J *et al.* (1996) Photosynthetic oxygen production and PAM fluorescence in the brown alga *Padina pavonica* (Linnaeus) Lamouroux measured in the field under solar radiation. *Marine Biology*, **127**, 61–66.

Hall-Spencer JM (2011) No reason for complacency. *Nature Climate Change*, **1**, 174.

Hall-Spencer JM, Rodolfo M, pa R *et al.* (2008) Volcanic carbon dioxide vents show ecosystem effects of ocean acidification. *Nature*, **454**, 96–99.

Harries DB, Harrow S, Wilson JR, Mair JM, Donnan DW (2007) The establishment of the invasive alga *Sargassum muticum* on the west coast of Scotland: a preliminary assessment of community effects. *Journal of the Marine Biological Association of the UK*, **87**, 1057–1067.

Hepburn CD, Pritchard DW, Cornwall CE, McLeod RJ, Beardall J, Raven JA, Hurd CL (2011) Diversity of carbon use strategies in a kelp forest community: implications for a high CO$_2$ Ocean. *Global Change Biology*, **17**, 2488–2497.

Hereu B (2006) Depletion of palatable algae by sea urchins and fishes in a Mediterranean subtidal community. *Marine Ecology Progress Series*, **313**, 95–103.

Hernández JC, Clement S, Sangil C, Brito A (2008) The key role of the sea urchin *Diadema* aff. *antillarum* in controlling macroalgae assemblages throughout the Canary Islands (eastern subtropical Atlantic): an spatio-temporal approach. *Marine Environmental Research*, **66**, 259–270.

Hillis-Colinvaux L (1980) Ecology and taxonomy of *Halimeda*: primary producer of coral reefs. *Advances in Marine Biology*, **17**, 1–327.

Hoffmann GE, Smith JE, Johnson KS *et al.* (2011) High-frequent dynamics of ocean pH: a multi-ecosystem comparison. *PLoS ONE*, **6**, doi: 10.1371/journal. pone.0028983.

Hoppe CJM, Langer G, Rokitta SD, Wolf-Gladrow DA, Rost B (2010) On CO$_2$ perturbation experiments: over-determination of carbonate chemistry reveals inconsistencies. *Biogeosciences Discussions*, **7**, 1707–1726.

IPCC (Intergovernmental Panel on Climate Change) (2007) Working Group 1 Report, The Physical Science Basis. Available at: http://www.ipcc.ch/publications_and_data/ar4/wg1/en/contents.html (accessed 1 March 2012).

Johnson VR, Brownlee , C *et al.* (2012) Responses of marine benthic microalgae to elevated CO$_2$. *Marine Biology*, doi: 10.1007/s00227-011-1840-2.

Kerrison P, Hall-Spencer JM, Suggett D, Hepburn LJ, Steinke M (2011) Assessment of pH variability at a coastal CO$_2$ vent for ocean acidification studies. *Estuarine, Coastal and Shelf Science*, **94**, 129–137.

Kleypas JA, Buddemeier RW, Archer D, Gattuso J-P, Langdon C, Opdyke BN (1999) Geochemical consequences of increased atmospheric carbon dioxide on coral reefs. *Science*, **284**, 118–120.

Kübler JE, Johnston AM, Raven JA (1999) The effects of reduced and elevated CO$_2$ and O$_2$ on the seaweed *Lomentaria articulata*. *Plant, Cell and the Environment*, **22**, 1303–1310.

Kuffner IB, Andersson AJ, Jokiel PL, Rodgers KS, Mackenzie FT (2008) Decreased abundance of crustose coralline algae due to ocean acidification. *Nature Geoscience*, **1**, 114–117.

Leinaas HP, Christie H (1996) Effects of removing sea urchins (*Strongylocentrotus droebachiensis*): stability of the barren state and succession of kelp forest recovery in the east Atlantic. *Oecologia*, **105**, 524–536.

Lewis E, Wallace WR (1998) *Program Developed for CO$_2$ System Calculations.* Carbon dioxide information analysis center, Oak Ridge National Laboratory, U.S. Department of Energy, Oak Ridge, TN.

Lewis SM, Norris JN, Searles RB (1987) The regulation of morphological plasticity in tropical reef algae by herbivory. *Ecology*, **68**, 636–641.

Ling SD, Ibbott S, Sanderson JC (2010) Recovery of canopy-forming macroalgae following removal of the enigmatic grazing sea urchin *Heliocidaris erythrogramma*. *Journal of Experimental Marine Biology and Ecology*, **395**, 135–146.

Littler MM, Littler DS (1980) The evolution of thallus form and survival strategies in benthic marine macroalgae: field and laboratory tests of a functional form model. *American Naturalist*, **116**, 25–44.

Martin S, Gattuso J-P (2009) Response of Mediterranean coralline algae to ocean acidification and elevated temperature. *Global Change Biology*, **15**, 2089–2100.

Martin S, Rodolfo M, pa R *et al.* (2008) Effects of naturally acidified seawater on seagrass calcareous epibionts. *Biology Letters*, **4**, 689–692.

Martone PT (2010) Quantifying growth and calcium carbonate deposition of *Calliarthron cheilosporiodes* (Corallinales, Rhodophyta) in the field using a persistent vital stain. *Journal of Phycology*, **46**, 13–17.

McClanahan TR (1994) Kenyan coral reef lagoon fish: effects of fishing, substrate complexity, and sea urchins. *Coral Reefs*, **13**, 231–241.

McConnaghey T (1998) Acid secretion, calcification, and photosynthetic carbon concentrating mechanisms. *Canadian Journal of Botany*, **76**, 1119–1126.

McConnaughey AT, Whelan JF (1997) Calcification generates protons for nutrient and bicarbonate uptake. *Earth Science Reviews*, **42**, 95–117.

McManus JW, Polsenberg JF (2004) Coral–algal phase shifts on coral reefs: ecological and environmental aspects. *Progress in Oceanography*, **60**, 263–279.

Middelboe AL, Hansen PJ (2007) Direct effects of pH and inorganic carbon on macroalgal photosynthesis and growth. *Marine Biology Research*, **3**, 134–144.

Miles H, Widdicombe S, Spicer JI, Hall-Spencer JM (2007) Effects of anthropogenic seawater acidification on acid base balance in the sea urchin *Psammechinus miliaris*. *Marine Pollution Bulletin*, **54**, 89–9.

Milliman JD (1974) *Marine Carbonates*, pp. 1–375. Springer, Berlin, Germany.

Mumby PJ, Hedley JD, Zychaluk K, Harborne AR, Blackwell PG (2006) Revisiting the catastrophic die-off of the urchin *Diadema antillarum* on Caribbean coral reefs: fresh insights on resilience from a simulation model. *Ecological Modelling*, **196**, 131–148.

Nelson WA (2009) Calcified macroalgae-critical to coastal ecosystems and vulnerable to change: a review. *Marine and Freshwater Research*, **60**, 787–801.

Okazaki M, Pentecost A, Tanaka Y, Miyata M (1986) A study of calcium carbonate deposition in the genus *Padina* (Phaeophyceae, Dictyotales). *British Phycological Journal*, **21**, 217–24.

Orr JC, Fabry VJ, Aumont O *et al.* (2005) Anthropogenic ocean acidification over the twenty-first century and its impact on calcifying organisms. *Nature*, **437**, 681–686.

Padilla DK (1993) Rip-stop in marine algae: minimising the consequences of herbivore damage. *Evolutionary Ecology*, **7**, 634–644.

Porzio L, Buia MC, Hall-Spencer JM (2011) Effects of ocean acidification on macroalgal communities. *Journal of Experimental Marine Biology and Ecology*, **400**, 278–287.

Price NN, Hamilton SL, Tottell JS, Smith JE (2011) Species-specific consequence of ocean acidification for the calcareous tropical green algae *Halimeda*. *Marine Ecology Progress Series*, **440**, 67–78.

R Development Core Team R (2011) *A Language and Environment for Statistical Computing.*

Ralph PJ, Gademan R (2005) Rapid light curves: a powerful tool to assess photosynthetic activity. *Aquatic Botany*, **82**, 222–237.

Raven R (2011) Effects on marine algae of changed seawater chemistry with increasing Atmospheric CO$_2$. *Biology and Environment: Proceedings of the Royal Irish Academy*, **111B**, 1–17.

Raven JA, Johnston AM, Kübler JE *et al.* (2002) Mechanistic interpretation of carbon isotope discrimination by marine macroalgae and seagrasses. *Functional Plant Biology*, **29**, 355–378.

Reiskind JB, Seamon PT, Bowes G (1988) Alternative methods of photosynthetic carbon assimilation in marine macroalgae. *Plant Physiology*, **87**, 686–692.

Riebesell U (2008) Acid test for marine biodiversity. *Nature*, **454**, 46–47.

Ritchie R (2006) Consistent sets of spectrophotometric chlorophyll equations for acetone, methanol and ethanol solvents. *Photosynthesis Research*, **89**, 27–41.

Robbins LL, Knorr PO, Hallock P (2009) Response of *Halimeda* to ocean acidification: field and laboratory evidence. *Biogeosciences Discussions*, **6**, 4895–4918.

Rodolfo M, pa R, Houlbrèque F *et al.* (2011) Coral and mollusc resistance to ocean acidification adversely affected by warming. *Nature Climate Change*, **1**, 308–312.

Roleda MY, Morris JN, McGraw CM, Hurd CL (2011) Ocean acidification and seaweed reproduction: increased CO$_2$ ameliorates the negative effect of lowered pH on meiospore germination in the giant kelp *Macrocystis pyrifera* (Laminariales, Phaeophyceae). *Global Change Biology*, **18**, 854–864.

Roy RN, Vogel KM, Porter-Moore C, Pearson T, Good CE, Millero FJ, Campbell DM (1993) The dissolution of constants of carbonic acid in seawater at salinities 5 to 45 and temperatures 0 to 45 °C. *Marine Chemistry*, **4**, 249–267.

Russell BD, Thompson J-AI, Falkenberg LJ, Connell SD (2009) Synergistic effects of climate change and local stressors: CO$_2$ and nutrient-driven change in subtidal rocky habitats. *Global Change Biology*, **15**, 2153–2162.

Russell BD, Harley CDG, Wernberg T, Mieszkowska N, Widdicombe S, Hall-Spencer JM (2011a) Predicting ecosystem shifts requires new approaches that integrate the effects of climate change across entire systems. *Biology Letters*, **8**, 164–166.

Russell BD, Passarelli CA, Connell SD (2011b) Forecasted CO$_2$ modifies the influence of light in shaping subtidal habitat. *Journal of Phycology*, **47**, 744–752.

Sala E, Boudouresque CF, Harmelin-Vivien ML (1998) Fishing, trophic cascades, and the structure of algal assemblages: evaluation of an old but untested paradigm. *Oikos*, **82**, 425–439.

Sammarco PW (1982) Effects of grazing by *Diadema antillarum* Philippi (Echinodermata: Echinoidea) on algal diversity and community structure. *Journal of Experimental Marine Biology and Ecology*, **65**, 83–105.

Sammarco PW, Levington JS, Ogden JC (1974) Grazing and control of coral reef community structure by *Diadema antillarum* Philippi (Echinodermata:Echinoidea): a preliminary study. *Journal of Marine Research*, **32**, 47–53.

Semesi IS, Kangwe J, Björk M (2009) Alterations in seawater pH and CO_2 affect calcification and photosynthesis in the tropical coralline alga, *Hydrolithon* sp. (Rhodophyta). *Estuarine and Coastal Shelf Science*, **84**, 337–341.

Sinutok S, Hill R, Doblin MA, Wuhrer R, Ralph PJ (2011) Warmer more acidic conditions cause decreased productivity and calcification in subtropical coral reef sediment-dwelling calcifiers. *Limnology and Oceanography*, **56**, 1200–1212.

Villouta E, Chadderton WL, Pugsley CW, Hay CH (2001) Effect of sea urchin (*Evechinus chloroticus*) grazing in Dusky Sound, Fiordland, New Zealand. *New Zealand Journal of Marine and Freshwater Research*, **35**, 1007–1024.

Wefer G (1980) Carbonate production by algae *Halimeda*, *Penicillus* and *Padina*. *Nature*, **285**, 323–324.

Wernberg T, Smale DA, Thomson MS (2012) A decade of climate change experiments on marine organisms: procedures, patterns and problems. *Global Change Biology*, **18**, 1491–1498

Widdicombe S, Spicer JI (2008) Predicting the impact of ocean acidification on benthic biodiversity: what can physiology tell us? *Journal of Experimental Marine Biology and Ecology*, **366**, 187–197.

Supporting Information

Additional Supporting Information may be found in the online version of this article:

Table S1. Seawater carbonate chemistry measurements for each study station off the island of Vulcano (V) and in Papua New Guinea; Upa-Upasina (U) and Esa'Ala (E), R= reference station, S = elevated CO_2 station. In Vulcano, temperature (range 18.6–27.7 °C), pH and salinity (= 38) were measured in Sept-Oct 2009, April 2010, July 2010, Sept-Oct 2010, May 2011, Sept–Oct 2011. In Papua New Guinea, temperature (range 28.2–31.4 °C), pH and salinity (= 34) were measured in April 2011. The pH and total alkalinity (Vulcano: mean TA, $n = 3$; PNG: median TA values taken from Fabricius *et al.*, 2011) were used to calculate the remaining parameters using CO_2 SYS programme (using the constants of Roy *et al.*, 1993 and Dickson, 1990 for KSO_4).

Table S2. Mean (± SE) abundance, length and width of aragonite crystals deposited by *Padina pavonica* along the Vulcano CO_2 gradient. Data derived from SEM analysis of fronds ($n = 3$ fronds per station), over calcified apical regions only (see frond images in Fig. 4), therefore do not reflect total means for whole fronds.

Please note: Wiley-Blackwell are not responsible for the content or functionality of any supporting materials supplied by the authors. Any queries (other than missing material) should be directed to the corresponding author for the article.